

# Evaluation of Transmit Diversity in MIMO-radar Direction Finding

Nikolaus H. Lehmann, *Student Member, IEEE*, Eran Fishler, *Member, IEEE*,  
Alexander M. Haimovich, *Senior Member, IEEE*, Rick S. Blum, *Fellow, IEEE*, Dmitry Chizhik,  
Leonard J. Cimini, Jr., *Fellow, IEEE*, and Reinaldo Valenzuela, *Fellow, IEEE*

## Abstract

It has been recently shown that multiple-input multiple-output (MIMO) antenna systems have the potential to dramatically improve the performance of communication systems over single antenna systems. Unlike beamforming, which presumes a high correlation between signals either transmitted or received by an array, the MIMO concept exploits the independence between signals at the array elements. In conventional radar, the target's radar cross section (RCS) fluctuations are regarded as a nuisance parameter that degrades radar performance. The novelty of MIMO radar is that it provides measures to overcome those degradations or even utilizes the RCS fluctuations for new applications. This paper explores how transmit diversity can improve the direction finding performance of a radar utilizing an antenna array at the receiver. To harness diversity, the transmit antennas have to be widely separated, while for direction finding, the receive antennas have to be closely spaced. The analysis is carried out by evaluating several Cramer Rao bounds for bearing estimation and the mean square error (MSE) of the maximum likelihood estimate.

## Index Terms

MIMO-radar, Cramer Rao bound, direction finding, array processing

**EDICS:** SAM-RADR, SAM-MCHA, OTH-EMRG

The work of A.M. Haimovich was supported by the Air Force Office of Scientific Research agreement no. FA9550-06-1-0026. The work of R.S. Blum is based on research supported by the Air Force Research Laboratory under agreement No. FA9550-06-1-0041.

Nikolaus H. Lehmann and Alexander M. Haimovich are with the New Jersey Institute of Technology, Newark, NJ 07102, USA (e-mail: lehmann, haimovich@njit.edu).

Eran Fishler is with Hite Capital Management, New York, NY 10016, USA (e-mail: eran@hitecapital.com).

Rick S. Blum is with the Lehigh University, Bethlehem, PA 18015, USA (e-mail: rblum@eecs.lehigh.edu).

Len Cimini is with the University of Delaware, Newark, DE 19716, USA (e-mail: cimini@ece.udel.edu).

Dmitry Chizhik and Reinaldo Valenzuela are with the Bell Laboratories - Lucent Technologies, Holmdel, NJ 07733, USA (e-mail: chizhik, rav@lucent.com).

## I. INTRODUCTION

Motivated by recent developments in communication theory, [1, 2], we explored the potentials of the multiple-input multiple-output (MIMO) concept in radar in [3, 4]. MIMO communication systems overcome the effect of fading in the wireless channel by transmitting redundant streams of data from several decorrelated transmitters [5]. For independent fading paths, the receiver of a MIMO system enjoys the fact that the average (over all information streams) signal to noise ratio (SNR) is more or less constant, as the number of paths increases, whereas in conventional systems, which transmit all their energy over a single path, the received SNR varies considerably.

In radar, a target is characterized by its radar cross section (RCS) function [6]. A target's RCS represents the amount of energy reflected from the target toward the receiver as a function of the target aspect with respect to the transmitter/receiver pair. It is well known that this function is rapidly changing as a function of the target aspect [6]. Both experimental measurements and modeling results demonstrate that scintillations of 20 dB or more in the reflected energy can occur by changing the target aspect by as little as one milliradian. These RCS scintillations are responsible for signal fading, which can cause large degradations in the system's detection and estimation performances.

Our proposed MIMO radar enjoys similar benefits to those enjoyed by MIMO communication systems. Specifically, the proposed approach overcomes target RCS fluctuations by transmitting different signals from several transmitters that illuminate the target from ideally decorrelated aspects. The received signal is a superposition of independently faded signals, and the average SNR of the received signal is more or less constant. This is in remarkable contrast to the conventional radar that suffers under large variations in the received power of target models according to Swerling case 1 and 3, respectively. Similar to communications, we may refer to this approach as *transmit diversity* and to the related performance improvement as *diversity gain*.

In Figure 1, the fluctuations in the energy reflected towards the angle  $\theta = 0$  are plotted versus the illumination angle. This figure is based on one realization of the statistical target model introduced later in this publication. With MIMO radar the target is illuminated from a set of angles. Therefore, the performance impairment found in conventional radar due to the drops in returned power at certain angles depicted in figure 1 are countervailed.

In [4], the improvements in detection performance with MIMO radar have been discussed. In [3], the impact of transmit diversity on the error of direction finding techniques has been explored by theoretical considerations based on the average Cramer Rao bound (CRB) and simulation results. The work presented here extends the latter publication by introducing the outage CRB and addressing the case of correlated target aspects.

MIMO radar can be viewed a generalization of multistatic radar setups. Receive diversity is considered in [7] for multistatic radar. The author discusses optimal processing of the received signals, but does not explore the diversity gain as such. Transmit diversity for multistatic sonar is, for example, analyzed in [8]. But the diversity is discussed with respect to different types of background noise and different propagation paths and not with respect to target aspects. Using several separated transmitters in a multistatic radar is proposed in e.g. [9]. However, the motivation to distribute the illumination sources is to hide them rather than achieve diversity.

Generally speaking, multistatic radar is considered an extension of bistatic radar or a network of several monostatic

radars. Among the motivations for multistatic radars found in the literature are the rejection of false targets due to reflections of a real target on some clutter, e.g. [10]. Normally this involves processing at each receiver and some fusion of the processed data at a central processor [11]. In contrast, we use the notion of MIMO radar to describe a system in which the target is illuminated by one or several sources seeking to exploit the angular diversity of the target. The system evaluates the received signals at the multiple receivers *jointly*.

It should be mentioned that the acronym MIMO has been used in the radar context by other authors, too, e.g. [12, 13]. But, the systems discussed generally consist of closely spaced elements, which therefore, do not capitalize on the target angular diversity. Rather, spatial filtering is achieved similar to regular beamforming.

Our notion of MIMO radar is not limited to diversity to overcome target fades. Later in this article, we introduce the channel matrix  $\mathbf{H}$ . It can be argued that the rank of this matrix relates to the complexity of the target, meaning the number of individual scatterers, and the target size. Further, the RCS fluctuations may be viewed as a *signature* of a target or a unique pattern. By sampling this pattern with a MIMO radar system it might be possible to classify targets. This may seed novel approaches for, e.g., spatial automatic target recognition. Topics like these lie within the current research activities of our group.

This paper explores the diversity gain for one particular scenario. For simplicity, we ignore target range and velocity and focus on the angle of arrival (AOA). The advantages of MIMO radar are demonstrated by comparing the possible and achieved precision of direction finding approaches. For the purpose of our analysis, we consider the problem of estimating the AOA of a single target illuminated by one or several sources. The latter may be considered an extension of the classical active direction finding (DF) problem in radar or sonar, [14, 15]. For direction finding, an array of closely spaced antennas is employed at the receive side to enable unambiguous angle estimation, [16- 18]. As mentioned previously, the MIMO radar system under consideration illuminates the target from several separated angles. The amount of energy reflected towards the receiver array is a function of the illumination angle, as Figure 1 illustrates. Figure 1 is one realization of the target model used here. Depending on the kind of target and the orientation of the target towards the transmitter/receiver pair the returned energy fluctuates. Thus, if the target is illuminated from a specific angle the return might almost vanish. However, if several sufficiently separated transmitters are employed and their signals are combined at the receive side, the total returned signal power from the target becomes approximately independent from the individual illumination angles and target realization. This improves the angle estimation, as the reflected signal power is more stable and fluctuates less. The resulting performance improvement is called *diversity gain*.

Let us reiterate, that in this publication, we discuss spatial diversity. Similar diversity gain improvements can be achieved with frequency or temporal diversity. The latter is for example embedded in Swerling case 2 or 4 models.

In conventional radar an array of closely spaced transmit antennas, as in Electronic Steered Array (ESA) systems or in [12], is employed at the transmitter side. However, in our simplified scenario of a single target in a clutter free environment such an array does not provide any advantages over a single transmit antenna. Hence in this analysis, a comparison of MIMO to a single antenna system is sufficient.

The rest of this paper is organized as follows: In Section II we develop a signal and channel model for MIMO

radar and discuss the conditions and the effects of transmit diversity. In Section III we explore the possible diversity gains by evaluating the Cramer Rao bounds for DF approaches. In Section IV, we demonstrate the theoretical results of Section III with simulation results. Finally, we draw conclusions in Section V.

## II. MIMO RADAR SIGNAL MODEL

In this section, we describe a general signal model for the MIMO radar. The model focuses on the effect of the target spatial properties ignoring range and Doppler effects. The signal model separates the target effect from the effects of the antenna layouts and of the propagation between transmitters and target and between target and receivers. By doing so, it provides insight into the principles of MIMO radar. Especially, the model reflects how the target properties, its size etc., contribute to the dependency of the RCS on the aspect. This enables us to derive a condition for the separation among the MIMO antennas necessary to achieve independent fading across the different target aspects.

Not surprisingly, the radar MIMO signal and channel models are related to MIMO channel models for communications, for example [19]. The signal model developed here is sufficiently general that it can be used to describe both conventional radar systems and the proposed MIMO radar system. Assume a MIMO radar system with two uniform linear arrays of  $M$  antennas at the transmitter and  $N$  antennas at the receiver. The transmitter and the receiver arrays are not necessarily collocated (bistatic radar). Assume also a far field complex target that consists of many, say  $Q$ , independent scatterers. The target is illuminated by narrowband signals, whose amplitudes do not change appreciably across the target. This means roughly a bandwidth smaller than  $c/D$ , where  $c$  is the speed of light and  $D$  is the target length. Each scatterer is assumed to have isotropic reflectivity modeled by zero-mean, unit-variance per dimension, independent and identically distributed (i.i.d.) Gaussian complex random variables  $\zeta_q$ . The target is then modeled by the diagonal matrix

$$\Sigma = \frac{1}{\sqrt{2Q}} \begin{pmatrix} \zeta_0 & 0 & \cdots & 0 \\ 0 & \zeta_1 & \ddots & \vdots \\ \vdots & \ddots & \ddots & 0 \\ 0 & \cdots & 0 & \zeta_{Q-1} \end{pmatrix}, \quad (1)$$

where the normalization factor makes the target average RCS  $E[\text{trace}(\Sigma\Sigma^H)] = 1$  independent of the number of scatterers in the model<sup>1</sup>. If the RCS fluctuations are fixed during an antenna scan, but vary independently from scan to scan, our target model represents a classical Swerling case 1 (which represents a target in slow motion) [6].

For simplicity, we assume that the target scatterers are laid out as a linear array, and that this array and the arrays at the transmitter and receiver are parallel. Figure 2 illustrates the model.

The signals radiated by the  $M$  transmit antennas impinge on the  $Q$  scatterers at angles  $\phi_{m,q}$ ,  $q = 0, \dots, Q - 1$  and  $m = 0, \dots, M - 1$  (measured with respect to the normal to the arrays). Assuming that the length of the target array is small compared to the distance, the signal transmitted by the  $m$ -th transmit antenna arrives as a planewave

<sup>1</sup>The superscript  $H$ , as in  $\Sigma^H$ , denotes the Hermitian transposed.

at the target. Thus, the angle of arrival at the target is independent from the scatterer,  $\phi_{m,q} = \phi_m, \forall q$ . The signal vector induced by the  $m$ -th transmit antenna is given by

$$\mathbf{g}_m = \left[ 1, e^{-j2\pi \sin \phi_m \Delta_2 / \lambda}, \dots, e^{-j2\pi \sin \phi_m \Delta_Q / \lambda} \right]^T, \quad (2)$$

where  $\Delta_q$  is the spacing between the first and  $(q+1)$ -th scatterer,  $\lambda$  is the carrier wavelength, and the superscript  $T$  denotes vector/matrix transposition. We further assume, that the target scatterers are uniformly spaced, i.e.,  $\Delta_q = q \cdot \Delta$ . Therefore, the vector  $\mathbf{g}_m$  describes the different phase-shifted versions of the signal transmitted by the  $m$ -th transmitter arriving at the different scatterers.

The signals are reflected by the target scatterers towards the receiver array elements at angles  $\theta_{n,q}, n = 0, \dots, N-1$  and  $q = 0, \dots, Q-1$ . Assuming that both the sizes of the target and the receiver arrays are small compared to the distance between them, we find that  $\theta_{n,q} = \theta$ . The signals reflected by the scatterers have in the far field, relative phase shifts described by the vector  $\mathbf{k}(\theta)$ ,

$$\mathbf{k}(\theta) = \left[ 1, e^{j2\pi \sin \theta \Delta / \lambda}, \dots, e^{j2\pi \sin \theta (Q-1) \Delta / \lambda} \right]^T. \quad (3)$$

A planewave signal arriving at the array at the angle  $\theta$  excites the elements of the array with phase shifts given by the vector  $\mathbf{a}(\theta)$ ,

$$\mathbf{a}(\theta) = \left[ 1, e^{-j2\pi \sin \theta d_r / \lambda}, \dots, e^{-j2\pi \sin \theta (N-1) d_r / \lambda} \right]^T, \quad (4)$$

where  $d_r$  denotes the inter element spacing at the receiver. We assume in the following a spacing of  $d_r = \lambda/2$  to enable unambiguous direction finding.

With the vectors and the target matrix defined above, we can express the received signals which originate from the  $m$ -th transmitter and are reflected by the target:

$$\mathbf{r}'_m = \mathbf{a}(\theta) \mathbf{k}^T(\theta) \mathbf{\Sigma} \mathbf{g}_m b_m s_m \quad (5)$$

The terms  $b_m$  are complex variables representing the phase shifts between the signals coming from different transmitters due to the different propagation delays. Without loss of generality, these phase shifts can be embedded in  $\mathbf{g}_m$ . The complex scalar  $s_m$  represents the component of the sampled receive filter output due to the waveform transmitted by the  $m$ -th transmitter. Organizing those scalars in the vector  $\mathbf{s} = [s_0, \dots, s_M]^T$ , we can describe the received signal as:

$$\begin{aligned} \mathbf{r} &= \mathbf{a}(\theta) \mathbf{k}^T(\theta) \mathbf{\Sigma} \sum_{m=0}^{M-1} \mathbf{g}_m s_m + \mathbf{v} \\ &= \mathbf{K} \mathbf{\Sigma} \mathbf{G} \mathbf{s} + \mathbf{v} \\ &= \mathbf{H} \mathbf{s} + \mathbf{v} \end{aligned} \quad (6)$$

The vector  $\mathbf{r} = [r_1, \dots, r_{N-1}]^T$  contains the sampled output of the filters at the  $N$  receiver elements,  $\mathbf{v}$  represents the additive Gaussian noise terms at the receivers after the receive filters. We assume that the noise components among the receivers are i.i.d. .

Further, the matrix  $\mathbf{K} = \mathbf{a}(\theta)\mathbf{k}^T(\theta)$  represents the propagation paths from the scatterers to the receivers, and the matrix  $\mathbf{G} = [\mathbf{g}_0, \dots, \mathbf{g}_{M-1}]$  the ones from the transmitters to the individual target scatterers. The  $N \times M$  matrix  $\mathbf{H}$  incorporates the paths from all transmitters to all receivers. The effect of the vector  $\mathbf{k}(\theta)$  is to combine the signals coming from the individual scatterers in the far field. As we assume that  $\Sigma$  consists of complex-valued random scatterers, the effect of  $\mathbf{k}(\theta)$  can be embedded in  $\Sigma$  and  $\mathbf{k}(\theta)$  can be replaced with  $\mathbf{1}_Q = [1, \dots, 1]^T$ , without loss of generality.

To achieve spatial diversity, it is required that different transmit antennas see uncorrelated aspects of the target. Let us consider again the received signal components due to the  $m$ -th transmitter:

$$\mathbf{r}'_m = \frac{1}{\sqrt{2}} \mathbf{a}(\theta) \alpha_m s_m \quad (7)$$

Here, we summarize the target fading effect to the fading coefficient  $\alpha_m$  given by  $\alpha_m = \sqrt{2} \mathbf{1}_Q^T \Sigma \mathbf{g}_m$ . The factor  $\sqrt{2}$  is introduced here so that the  $|\alpha_m|^2$  random variables have a  $\chi_2^2$  distribution, which will ease later considerations. The previously mentioned uncorrelated target aspects result in uncorrelated fading coefficients. As the fading coefficients are modeled as zero mean and independent, we find  $E\{\alpha_m^* \alpha_{m+1}\} = 0$ , which leads to

$$\begin{aligned} E\{\alpha_m^* \alpha_{m+1}\} &= E\{\mathbf{g}_m^H \Sigma^H \mathbf{1}_Q \mathbf{1}_Q^T \Sigma \mathbf{g}_{m+1}\} \\ &= \mathbf{g}_m^H E\{\Sigma^H \mathbf{1}_Q \mathbf{1}_Q^T \Sigma\} \mathbf{g}_{m+1} \\ &= \frac{1}{2Q} \mathbf{g}_m^H \mathbf{I}_Q \mathbf{g}_{m+1} = 0. \end{aligned} \quad (8)$$

Thus, the fading constants for the different transmitters are uncorrelated if the columns of  $\mathbf{G}$  are orthogonal:

$$\mathbf{g}_m^H \mathbf{g}_{m+1} = \sum_{q=0}^{Q-1} e^{j2\pi[(\sin \phi_{m+1} - \sin \phi_m)q\Delta/\lambda]} = 0 \quad (9)$$

For small angles  $\phi_m$  and  $\phi_{m+1}$  expressed in radians, we approximate the difference of the sine terms in (9) with

$$\sin \phi_{m+1} - \sin \phi_m \approx d_t/R, \quad (10)$$

where  $d_t$  is the inter-element spacing at the transmitter and  $R$  is the distance between the target and the transmitter.

Using this in (9), we obtain

$$\sum_{q=0}^{Q-1} e^{j2\pi(d_t/R)q\Delta/\lambda} = 0. \quad (11)$$

Thus, orthogonality is achieved when the angles complete one turn in the complex plane:

$$\frac{d_t \Delta}{\lambda R} = \frac{1}{Q} \quad (12)$$

However, for large values of  $Q$  and for

$$\frac{d_t \Delta}{\lambda R} \geq \frac{1}{Q} \quad (13)$$

the orthogonality condition (11) is approximately met. A similar argument is made in [19]. This condition obtained solely from geometric considerations has an appealing intuitive physical interpretation. The beamwidth of the energy backscattered from the target towards the transmitter is approximately given by  $\lambda/D$ , where  $D = Q \cdot \Delta$  is the

target size. The target presents different aspects to adjacent transmit antennas if the inter-element spacing at the transmitter is greater than the target beamwidth coverage at distance  $R$ , namely

$$d_t \geq \frac{\lambda R}{D}, \quad (14)$$

which turns out to be the same as (13). We note, that the here presented target model is rather simple. However, its main purpose is to derive a condition for independent fading coefficients over the target. In [4] we presented a more sophisticated model with a continuous 2-dimensional scatterer distribution, which results in the same condition, (14). In contrast to [4], we explore in this publication the effect of correlated fading coefficients and target aspects in section IV-A, too.

#### A. Model Classification

MIMO radar signal models can be classified into three general groups:

- Conventional radar array modeled with an array at the receiver and a single antenna or an array at the transmitter. The array elements are spaced at half-wavelengths to enable beamforming and DF.
- MIMO radar for DF. Transmit antenna elements are widely spaced to support spatial diversity with respect to the aspects of the target. The receiver array performs DF.
- MIMO radar with widely separated antennas at both the transmitter and the receiver.

This paper discusses the first two signal models, whereas the third one is discussed in [4].

1) *Conventional Radar Array*: Conventional radar arrays are systems in which the elements of the transmitting and receiving arrays are closely spaced. At the transmitter, that means that the inter-element spacing does not meet (13) or, equivalently, that multiple elements are contained within one target beamwidth. At the receiver, the spacing is  $d_r \leq \lambda/2$  to enable unambiguous estimation of the angle of arrival.

Let the target bearings with respect to the transmit and receive arrays be  $\phi$  and  $\theta$ , respectively. The term  $b_m$  in (5) is given by  $b_m = e^{-2\pi \sin \phi m d_t / R}$ . As mentioned before, we can neglect those phase shifts in the MIMO scenario. However for conventional radar we include them in the related expression to accommodate the eventual use of ESAs at the transmitter site. The phase shifts are collected in the vector  $\mathbf{b}(\phi)$ . The transmit matrix is given by  $\mathbf{G} = \mathbf{1}_Q \mathbf{b}^T(\phi)$ . The receive matrix is given by  $\mathbf{K} = \mathbf{a}(\theta) \mathbf{1}_Q^T$ . We note, that actually  $\mathbf{G}$  and  $\mathbf{K}$  should both contain the vectors  $\mathbf{g}(\phi)$  and  $\mathbf{k}(\theta)$ , respectively. However, as those vectors are constant for all receiver and transmitter elements and because of the randomness of the  $\mathbf{\Sigma}$  matrix, we replace them with  $\mathbf{1}_Q$  without losing any insight. It follows that the channel matrix is given by

$$\begin{aligned} \mathbf{H} &= \mathbf{a}(\theta) \mathbf{1}_Q^T \mathbf{\Sigma} \mathbf{1}_Q \mathbf{b}^T(\phi) \\ &= \frac{1}{\sqrt{2}} \alpha \mathbf{a}(\theta) \mathbf{b}^T(\phi), \end{aligned} \quad (15)$$

where the fading coefficient is  $\alpha = \sqrt{2} \cdot \mathbf{1}_Q^T \mathbf{\Sigma} \mathbf{1}_Q$ . By assumption, the elements of  $\mathbf{\Sigma}$ ,  $\zeta_q$  (see (1)), are zero-mean, unit-variance per dimension, i.i.d. Gaussian random variables. Hence,  $\alpha$  is a zero-mean, complex Gaussian random

variable, too. Subsequently, the target's RCS  $|\alpha|^2$ , follows a  $\chi_2^2$  chi-square distribution with 2 degrees of freedom. Note that with this model, there is no diversity 'gain' in the target RCS.

The beamforming of a conventional radar array on the transmit side is represented by the vector  $\mathbf{b}^*(\phi')$ . As the transmitter elements radiate the same waveform with different phases, the received signal can be expressed as

$$\mathbf{r} = \frac{1}{\sqrt{2}} \mathbf{a}(\theta) \mathbf{b}^T(\phi) \mathbf{b}^*(\phi') \alpha s + \mathbf{v}, \quad (16)$$

where  $s$  is a scalar representing the filter outputs due to the single transmitted waveform. Now, if the receiver uses a beamformer to steer towards direction  $\theta'$ , then the output of the beamformer processing is

$$\begin{aligned} y &= \mathbf{a}^H(\theta') \mathbf{r} + \mathbf{v}' \\ &= \frac{1}{\sqrt{2}} \mathbf{a}^H(\theta') \mathbf{a}(\theta) \mathbf{b}^T(\phi) \mathbf{b}^*(\phi') \alpha s + \mathbf{v}'. \end{aligned} \quad (17)$$

This model represents a bistatic radar where  $\mathbf{b}^T(\phi) \mathbf{b}^*(\phi')$  plays the role of the transmit antenna pattern, whereas  $\mathbf{a}^H(\theta') \mathbf{a}(\theta)$  is the receive antenna pattern. The angle of arrival is estimated as the  $\theta'$  which maximizes  $|y|^2$ . The target component, which maximizes  $|y|^2$  at the estimated angle of arrival, is subject to fading due to the  $|\alpha|^2$  multiplier. In the scenario considered here, which equals the Swerling I case, this fading gain has a  $\chi_2^2$  distribution (chi-square with 2 degrees of freedom).

2) *MIMO Radar - Direction Finding*: In MIMO radar for direction finding (DF), the transmit antennas are sufficiently separated to meet the orthogonality condition (13) for targets of interest. Equivalently, the columns of the transmit matrix  $\mathbf{G}$  meet the orthogonality condition in (9). In contrast, elements of the receive array are closely separated to enable DF measurements. Assume that the target is at angle  $\theta$  with respect to the receive array normal. The receive matrix is given by  $\mathbf{K} = \mathbf{a}(\theta) \mathbf{1}_Q^T$ . From (6), it follows that the channel matrix is given by

$$\mathbf{H} = \frac{1}{\sqrt{2}} \mathbf{a}(\theta) \boldsymbol{\alpha}^T, \quad (18)$$

where the components  $\alpha_m$  of the  $M \times 1$  vector  $\boldsymbol{\alpha}$ , are the previously introduced target fading coefficients for each target illuminating path,  $\alpha_m = \sqrt{2} \cdot \mathbf{1}_Q^T \boldsymbol{\Sigma} \mathbf{g}_m$ . Thus, the vector  $\boldsymbol{\alpha}$  is given as  $\boldsymbol{\alpha} = \sqrt{2} \cdot (\mathbf{1}_Q^T \boldsymbol{\Sigma} \mathbf{G})^T$ . Due to the orthogonality among the transmit vectors  $\mathbf{g}_m$ , the variates  $\alpha_m$  are uncorrelated. Moreover, the random variables  $\alpha_m$  are zero-mean, unit-variance (per dimension), independent, identical distributed (i.i.d.) complex normal.

The signal model is given by

$$\begin{aligned} \mathbf{r} &= \frac{1}{\sqrt{2}} (\mathbf{a}(\theta) \boldsymbol{\alpha}^T) \mathbf{s} + \mathbf{v} \\ &= \frac{1}{\sqrt{2}} \mathbf{a}(\theta) \sum_{i=0}^{M-1} \alpha_i s_i + \mathbf{v}. \end{aligned} \quad (19)$$

Assuming that the total transmission power is independent of the number of transmitters, e.g.

$\sum_{i=0}^{M-1} E\{|s_i|^2\} = 1$ , the signal model, with all normalization factors specified so far, ensures that the average received power  $E\left\{\left|(1/\sqrt{2}) \sum_{i=0}^{M-1} \alpha_i s_i\right|^2\right\} = 1$ . Conditioned on the fading constants vector  $\boldsymbol{\alpha}$  and the signal vector  $\mathbf{s}$ , the received vector  $\mathbf{r}$  is complex, multivariate normal with correlation matrix  $\frac{1}{2} \|\boldsymbol{\alpha}^T \mathbf{s}\|^2 \mathbf{a}(\theta) \mathbf{a}^H(\theta) + 2\sigma^2 \mathbf{I}_N$ .

To illustrate how the considered system utilizes diversity, we assume here  $M = 2$ . First we analyze the properties of one signal and its power at a single receiver element ignoring the phase shifts along the array:

$$\begin{aligned} r &= \frac{1}{\sqrt{2}}(\alpha_0 s_0 + \alpha_1 s_1) + v \\ |r|^2 &= \frac{1}{2}|\alpha_0 s_0 + \alpha_1 s_1 + v|^2 \end{aligned} \quad (20)$$

The diversity cannot be utilized in this manner, as the signal components  $s_i$  might destructively interfere with each other, since the fading coefficients  $\alpha_i$  are unknown *a priori*. To prevent this effect, orthogonal waveforms can be employed. However, in this publication, we assume that the transmitted waveforms result in random and mutually independent components,  $s_i$ , of the sampled receive filter outputs. Evaluating the expectation of the received signal power, we find:

$$\begin{aligned} E\{|r|^2\} &= E\left\{\left|\frac{1}{\sqrt{2}}(\alpha_0 s_0 + \alpha_1 s_1) + v\right|^2\right\} \\ &= \frac{1}{4}(|\alpha_0|^2 + |\alpha_1|^2) + 2\sigma^2, \end{aligned} \quad (21)$$

where we assumed  $E\{|s_i|^2\} = \frac{1}{2}$ . In the considered scenario, the angle of arrival estimate is based on a sufficiently large number of snapshots during which the fading coefficients are assumed to be constant. The waveforms of each transmitter result in a different random output component for each snapshot. Thus, when the number of snapshots is sufficiently large, we may approximate the sum over the received power as

$$\begin{aligned} \sum_{i=0}^{L-1} |r_i|^2 &= \sum_{l=0}^{L-1} \left|\frac{1}{\sqrt{2}}(\alpha_0 s_{0,l} + \alpha_1 s_{1,l}) + v_l\right|^2 \\ &\approx \frac{1}{4}(|\alpha_0|^2 + |\alpha_1|^2)L\hat{s}^2 + 2L\hat{\sigma}^2, \end{aligned} \quad (22)$$

where  $\hat{s}^2$  and  $\hat{\sigma}$  indicate, that these values are estimates of the (single) signal and noise power, which are random variables. In the remainder of this publication, we assume that a sufficiently large number of snapshots is processed, and that therefore the power of the target component is determined by the (scaled) sum of the squared absolute values of the fading coefficients. Including the array on the receive side, we may write for the vector of the received samples along the array:

$$\mathbf{r} = \mathbf{a}(\theta) \frac{1}{\sqrt{2}}(\alpha_0 s_0 + \alpha_1 s_1) + \mathbf{v} \quad (23)$$

To estimate the angle of arrival over several snapshots, the following expression is evaluated:

$$\begin{aligned} \xi(\theta') &= \sum_{l=0}^{L-1} |\mathbf{a}(\theta') \mathbf{r}_l|^2 = \sum_{l=0}^{L-1} |\mathbf{a}^H(\theta') \mathbf{a}(\theta) \frac{1}{\sqrt{2}}(\alpha_0 s_{0,l} + \alpha_1 s_{1,l}) + \mathbf{a}^H(\theta') \mathbf{v}_l|^2 \\ &\approx |\mathbf{a}^H(\theta') \mathbf{a}(\theta)|^2 \frac{1}{4}(|\alpha_0|^2 + |\alpha_1|^2) L\hat{s}^2 + LN\hat{\sigma}^2 \end{aligned} \quad (24)$$

The angle of arrival is estimated as the  $\theta'$  which maximizes  $\xi(\theta')$ . For the correct estimate  $\theta' = \theta$  the term  $|\mathbf{a}^H(\theta') \mathbf{a}(\theta)|^2$  equals  $N^2$ . Again, the target component in this estimation is subject to fading. However, the fading is due to the *sum* of  $|\alpha_0|^2$  and  $|\alpha_1|^2$ . As the random variables  $|\alpha_i|^2$ ,  $i = 0, 1$ , have a  $\chi_2^2$  distribution, and they

are i.i.d. (due to the orthogonality between  $\mathbf{g}_0$  and  $\mathbf{g}_1$ ), their sum in (24) has a  $\chi_4^2$  (chi-square with 4 degrees of freedom) distribution. This is a consequence of the different, uncorrelated RCS's presented by the target to the different elements of the transmitting array. Due to the scaling in (24) and (17) the average signal power reflected by the target is in both cases 1. The reflected power is in the conventional radar case, (17), a scaled  $\chi_2^2$  random variable; whereas it is a scaled  $\chi_4^2$  random variable in the MIMO scenario, (24). The latter has a smaller variance than the first. Thus, the *diversity* results in a more advantageous distribution of the target component in the received signal. The resulting performance improvement is called *diversity gain* and is explored by different means in the following sections.

Assuming that the different transmit signals result in i.i.d. Gaussian random variables after the receive filters facilitates the mathematical analysis carried out in the next section. Moreover, this assumption keeps the derived results general without limiting the discussion to particular transmit waveforms or signals. One of our current research topics is to find more evolved waveforms suitable for MIMO radar. However, apart from the resulting analytical tractability and generality, the assumption applies to passive radar systems using *sources of opportunity*, e.g. [20, 21], to estimate the bearing of targets without knowledge of the specific transmitted signals and waveforms.

### III. MIMO DF ANALYSIS

In this section, we examine the performance of a MIMO radar when used as a DF system. For simplicity and mathematical tractability, we make the following assumptions:

- 1) Several, independent snapshots of the target are available for processing.
- 2) The transmitted waveforms result in components of the receive filter output summarized in the vector  $\mathbf{s}$  for each snapshot. The vector is modeled as Gaussian random with independent components. Thus, the effective illumination process is spatially white and its correlation matrix is  $(1/M) \mathbf{I}_M$ .
- 3) The antenna elements of both the transmitting and the receiving arrays are omnidirectional.
- 4) Since we are interested in a DF application, without loss of generality we assume that the signals from the different transmitters arrive synchronized at the receiver.

A common figure of merit for comparing the performance of different systems is the estimators' mean square error (MSE). A system's MSE depends on the exact estimation method, e.g., ML, MUSIC, beamforming, used. In order to have a fair comparison between different systems we evaluate the Cramer Rao bound, which serves as a lower bound on the performance of all unbiased estimators.

#### A. Cramer Rao Bound

In what follows, we analyze the performance of a MIMO radar used as an active direction finder with  $M \geq 1$  transmitting elements. The received signal is given by the model (19). In our model there are three unknown parameters, the direction parameter  $\theta$ , the target's fading parameters contained in  $\boldsymbol{\alpha} = [\alpha_0, \dots, \alpha_{M-1}]^T$ , and the noise power  $\sigma^2$ . The vector containing all the unknown parameters is  $\boldsymbol{\psi} = [\theta, \sigma^2, \boldsymbol{\alpha}]$ . We let  $f(\mathbf{r}|\boldsymbol{\psi})$  denote the family of probability density functions (pdf) of the received signal parameterized by the vector of unknown

parameters in  $\boldsymbol{\psi}$  and  $\mathbf{C}(\boldsymbol{\psi})$  the correlation matrix of the error in estimating  $\boldsymbol{\psi}$  of any unbiased estimator. The Cramer-Rao lower bound for estimating  $\boldsymbol{\psi}$  is given by

$$\mathbf{C}(\boldsymbol{\psi}) \geq \text{CRB}(\boldsymbol{\psi}) = \mathbf{J}^{-1}(\boldsymbol{\psi}) = \left( -E \left\{ \frac{\partial^2 \ln f(\mathbf{r}|\boldsymbol{\psi})}{\partial \boldsymbol{\psi} \partial \boldsymbol{\psi}^T} \right\} \right)^{-1}. \quad (25)$$

The  $\geq$  indicates in this context, that the result of  $\mathbf{C}(\boldsymbol{\psi}) - \text{CRB}(\boldsymbol{\psi})$  is a positive definite matrix. This particularly implies  $\mathbf{C}_{1,1}(\boldsymbol{\psi}) \geq \text{CRB}_{1,1}(\boldsymbol{\psi})$ . We are interested only in the direction  $\theta$  and therefore the  $[1, 1]$  elements of  $\mathbf{C}(\boldsymbol{\psi})$  and  $\text{CRB}(\boldsymbol{\psi})$ , respectively. The other parameters are nuisance parameters. Particularly, we note that the problem decouples, which means that the estimation error of the AOA is independent of the estimation error of the signal and noise power. We let  $\text{CRB}(\theta|\boldsymbol{\alpha})$  denote the  $[1, 1]$  element of the Cramer Rao bound matrix. This notation indicates the conditioning of the bound on the unknown parameters in  $\boldsymbol{\alpha}$ . Given that the signals from the  $M$  transmitters are unknown complex Gaussian random variables with the correlation matrix  $(1/M)\mathbf{I}_N$  and conditioned on  $\boldsymbol{\alpha}$ ,  $\mathbf{r}$  is a complex normal random vector with correlation matrix  $\mathbf{C}_{\mathbf{r}} = (2M)^{-1} \|\boldsymbol{\alpha}\|^2 \mathbf{a}(\theta) \mathbf{a}^H(\theta) + 2\sigma^2 \mathbf{I}_N$ . We note here again, that  $\|\boldsymbol{\alpha}\|^2$  is  $\chi_{2M}^2$  distributed.

The CRB conditioned on the fading coefficients can be computed either by using expressions given in [22] or [23],

$$\text{CRB}(\theta|\boldsymbol{\alpha}) = \frac{6}{L\pi^2 \cos^2 \theta (N^2 - 1)} \left( \frac{2\sigma^2 2M}{N \|\boldsymbol{\alpha}\|^2} + \frac{(2\sigma^2)^2 4M^2}{N^2 \|\boldsymbol{\alpha}\|^4} \right) \quad (26)$$

where  $L$  is the number of snapshots used by the array for estimating  $\theta$ . This expression is based on assuming an Uniform Linear Array (ULA) at the receiver with an inter element spacing of  $\lambda/2$ . Therefore, the elements of the vector  $\mathbf{a}(\theta)$  are given by  $[\mathbf{a}(\theta)]_k = e^{j\pi \sin \theta k}$ .

### B. Average CRB

We can lower bound the average MSE of any unbiased estimator by averaging the CRB with respect to  $\boldsymbol{\alpha}$ . We denote this bound by  $\text{ACRB}(\theta) = E_{\boldsymbol{\alpha}}\{\text{CRB}(\theta|\boldsymbol{\alpha})\}$ . Using (26), the  $\text{ACRB}(\theta)$  is given by

$$\begin{aligned} \text{ACRB}(\theta) &= E_{\boldsymbol{\alpha}}\{\text{CRB}(\theta|\boldsymbol{\alpha})\} \\ &= \frac{6}{L\pi^2 \cos^2 \theta (N^2 - 1)} \left( \frac{2\sigma^2 2M}{N} E_{\boldsymbol{\alpha}} \left\{ \frac{1}{\|\boldsymbol{\alpha}\|^2} \right\} + \frac{(2\sigma^2)^2 4M^2}{N^2} E_{\boldsymbol{\alpha}} \left\{ \frac{1}{\|\boldsymbol{\alpha}\|^4} \right\} \right). \end{aligned} \quad (27)$$

Using

$$E_{\chi_{2M}^2} \left\{ \frac{1}{X} \right\} = \int_0^\infty \frac{x^{M-2} e^{-x/2}}{\Gamma(M) 2^M} dx = \frac{1}{2(M-1)} \quad \forall M > 1$$

and

$$E_{\chi_{2M}^2} \left\{ \frac{1}{X^2} \right\} = \int_0^\infty \frac{x^{M-2} e^{-x/2}}{\Gamma(M) 2^M} dx = \frac{1}{2^2(M-1)(M-2)}, \quad \forall M > 2$$

we find, that the  $\text{ACRB}$  is given by

$$\text{ACRB}(\theta) = \frac{6}{L\pi^2 \cos^2 \theta (N^2 - 1)} \left( \frac{2\sigma^2 M}{N(M-1)} + \frac{(2\sigma^2)^2 M^2}{N^2(M-1)(M-2)} \right) \quad \forall M > 2. \quad (28)$$

Before investigating the dependency of the ACRB on the number of transmit antennas  $M$ , we explore some special cases of the parameters  $\theta$  and  $N$ .

$\theta \rightarrow \pi/2$ : Here  $\text{ACRB}(\theta) \rightarrow \infty$  confirms that the direction cannot be estimated at endfire, since the array has a zero effective aperture (zero resolution).

$\theta = 0$ : This is the best case for estimating the direction parameter. Indeed, at broadside the array has the largest effective aperture (best resolution). We assume in the following  $\theta = 0$  unless stated otherwise.

$N = 1$ : The bound is infinite. Indeed, a single omnidirectional antenna cannot measure the angle of arrival.

It is easy to verify that if the target's RCS is independent of the aspect, that is if  $\|\alpha\|^2 = 2M$  deterministically, the CRB is independent of  $M$ . Having this in mind, it is only natural to define the system's Fading Loss (FL) as the additional SNR necessary to achieve the same average MSE as a system, which is not subject to fading.

By taking the ratio of the ACRB given (28) and the unfaded CRB given by (26) with  $\|\alpha\|^2 = 2M$ , it is easy to verify that the fading loss (in dB) as a function of the number of elements in the transmitting array is lower and upper bounded as

$$10 \log_{10} \frac{M}{M-1} \leq \text{FL}(M) \leq 10 \log_{10} \frac{M}{\sqrt{(M-1)(M-2)}}. \quad (29)$$

For  $M \leq 2$  no finite expression for the ACRB can be found, as the unlimited error of the instantaneous CRB increases faster towards infinity than the probability weight function decreases towards zero for a decreasing  $\|\alpha\|^2$ . This means, that the integral related to evaluating  $E_X\{\frac{1}{X}\}$  does not converge when  $X$  is  $\chi_2^2$  distributed and the one related to  $E_X\{\frac{1}{X^2}\}$  does not converge when  $X$  is  $\chi_2^2$  or  $\chi_4^2$ . Therefore, the expressions in (28) and (29) are only valid for  $M \geq 3$ . As the integral does not converge to a finite value, the ACRB is infinite.

If we hypothetically consider  $M = 1$  and  $2$  in the expressions (28) and (29) we find that the ACRB as defined by (28) is infinite, too. Furthermore, we find that the lower and upper bound for the fading loss in (29) are infinite for  $M = 1$  and that for  $M = 2$  the upper bound for the fading loss is infinite. Thus, the expressions for the ACRB also reflect the behavior of the actual ACRB for  $M = 1$  and  $M = 2$ .

In contrast to the ACRB and its expressions, the average MSE of an unbiased estimator might be finite even for  $M = 1$  and  $2$ , when the unknown angle parameter  $\theta$  is estimated with, for example, the maximum likelihood approach. This discrepancy deserves additional consideration. The CRB bound is a small error bound. This means, it predicts the MSE based on the behavior of the log-likelihood function in the vicinity of the true parameter vector. As a small error bound, it ignores the full structure of the parameter space [23], which may result in nonsensical values. For example, in the problem at hand, if  $\|\alpha\|^2$  is small, the instantaneous CRB in (26), might be much larger than  $\pi^2$ . However, the MSE of any estimator is upper bounded by  $\pi^2$  for all values of  $\|\alpha\|^2$ . Thus, the average MSE of any estimator must be smaller than or equal to  $\pi^2$ . Hence in those cases, the ACRB is not related to the performance of any true estimator.

In the next section we introduce another way to evaluate the statistics of the instantaneous CRB which is capable of handling small values of  $M$ .

Now, consider the asymptotic case  $M \rightarrow \infty$ . Here, the fading loss approaches zero, that is, the target's RCS

'hardens' and is not subject to fluctuations. Without target fluctuations, a case referred to as Swerling case 5, the received signal is  $\mathbf{r} = \mathbf{a}(\theta)s + \mathbf{v}$ . The signal component at each receive element is then a Gaussian random variable with power  $|s|^2 = 1$ . With fluctuations, the received signal is  $\mathbf{r} = (1/\sqrt{2}) \mathbf{a}(\theta) \sum_{m=1}^M \alpha_m s_m + \mathbf{v}$ . The signal power at each receive element is then given by  $\sum_{m=0}^{M-1} |\alpha_m|^2 \frac{1}{2} \sigma_{s_m}^2$ , where the  $\sigma_{s_m}^2 = \frac{1}{M}$  is the transmit power of each illuminating antenna. As  $\sum_{m=0}^{M-1} |\alpha_m|^2$  is a  $\chi_{2M}^2$  random variable, the mean of the receive power is constantly 1 and the variance is  $\frac{1}{M}$ . Thus, as  $M$  tends towards infinity the variance of the instantaneous received signal power tends to 0 and the signal power becomes therefore deterministic.

Figure 3 illustrates the ACRB versus the SNR for  $M = 4, 16, \infty$ . The SNR refers to a single snapshot, thus it is the ratio  $E_{\alpha}\{(2M)^{-1} \|\alpha\|^2\} / 2\sigma^2$  in dB. Other parameters are set to  $N = 6$  receive antennas,  $\theta = 0$  angle of arrival, and  $L = 80$  snapshots.

We can see, that using 4 transmit antennas instead of 16 results in a fading loss of 1.3dB as predicted by (29). The *transmit diversity* alters the distribution of the received signal power. Even though the mean of the received signal power is the same for any number of transmit antennas, the smallest achievable average MSE of any estimator decreases with an increasing number of antennas. However, as the average is considered, the related diversity gains are not so tremendous as the ones in the next section.

### C. Outage CRB

In the previous section we found that the ACRB is not converging for  $M \leq 2$ . We introduce the *outage CRB* to enable the analysis for  $M = 1, 2$  transmit antennas. Moreover, similar to the outage analysis in communications, the outage CRB serves as a tool for analyzing *slow* fading target cases.

#### Definition: Outage CRB

If the CRB for the parameter to estimate  $\theta$  depends on the realization of a random variable  $\psi$ , we define the outage CRB for a given probability  $p$  as  $\text{CRB}_{out=p}(\theta)$ :

$$Pr\left\{\text{CRB}(\theta|\psi) \geq \text{CRB}_{out=p}(\theta)\right\} = p$$

In other words, with probability  $1 - p$  the random variable  $\psi$  has such a realization, that the lower bound of the MSE of any estimator is smaller than  $\text{CRB}_{out=p}$ . Therefore, it is not possible to find any estimator, which has an MSE of less than  $\text{CRB}_{out=p}$  with a probability  $p' > 1 - p$ .

As the CRB in (26) depends on the realization of  $\|\alpha\|^2$ , we find  $\text{CRB}_{out=p}$  for a given  $p$  as:

$$Pr\left\{\text{CRB}(\theta \|\alpha\|^2) \geq \text{CRB}_{out=p}(\theta)\right\} = p \quad (30)$$

As the CRB is strictly monotonic decreasing with  $\|\alpha\|^2$ , (30) indicates that we can find an  $\|\alpha_{out=p}\|^2$  so that

$$Pr\left\{\|\alpha\|^2 \leq \|\alpha_{out=p}\|^2\right\} = p \quad (31)$$

and therefore

$$\text{CRB}_{out=p}(\theta) = \text{CRB}(\theta \|\alpha_{out=p}\|^2). \quad (32)$$

For a given  $p$  and  $M$  the quantile  $\|\alpha\|_{out=p}^2$  can be found by evaluating the inverse of the  $\chi_{2M}^2$  probability distribution function numerically or by using tables in, e.g., [24]. The results presented in Figure 4 are based on the `chi2inv` function of Matlab.

Figure 4 shows  $\text{CRB}_{p=0.01}$  and  $\text{CRB}_{p=0.1}$  for different SNRs. We can see that the SNR gains depend on the probability  $p$ . In other words, when we want to compare  $M = 1, 4$  and  $16$  for  $\text{CRB}_{p=0.01}$  meaning that in 99 percent of the scenarios an estimator can achieve an MSE better than  $\text{CRB}_{p=0.01}$ , we find that for achieving those MSE's the case  $M = 1$  requires 13dB more SNR than  $M = 4$  and 17dB more than  $M = 16$ . Further, we see that in this case, the difference between  $M = 4$  and  $M = 16$  is 3dB compared to the 1.4dB in the previous ACRB analysis.

The transmit diversity has a stronger impact on the outage CRB for small outages than on the ACRB, as the outage CRB is related to the tails of the distributions of  $\frac{1}{\|\alpha\|^2}$  and  $\frac{1}{\|\alpha\|^4}$  whereas the ACRB is related to their means. As stated earlier, the diversity reduces the variance of the of the received signal power, which makes the chance small, that the signal component almost vanishes due to the target fading.

#### IV. SIMULATION RESULTS

In this section, we explore the MSE and the estimation error distribution of the ML- estimator. We assume a simplified scenario, in which the signals originating from the different transmitters arrive synchronized at the receiver, but are not known by the receiver. The received vector is then given by (6). We assume  $L = 80$  snapshots,  $\theta = 0$  and  $N = 6$ . The angle  $\theta$  is estimated at the receiver by maximizing the term  $\sum_{l=1}^L |\mathbf{a}^H(\theta') \mathbf{r}_l|^2$ , where  $\mathbf{r}_l$  is the received signal of the  $l$ -th snapshot. Thus, the estimated angle of arrival  $\hat{\theta}$  is:

$$\hat{\theta} \quad : \quad \sum_{l=1}^L |\mathbf{a}^H(\hat{\theta}) \mathbf{r}_l|^2 = \max_{\theta'} \sum_{l=1}^L |\mathbf{a}^H(\theta') \mathbf{r}_l|^2 \quad (33)$$

Figure 5 shows the (average) MSE for different SNR values and  $M = 1, 2, 4$  and  $16$ . We see that the curves for  $M = 4$  and  $M = 16$  are in excellent agreement with the curves in Figure 3. Thus, we can conclude, that in these scenarios the ML-estimator achieves the ACRB. Furthermore, for  $M = 1$  and  $2$ , the MLE provides a useful estimate of the angle of arrival, even though the expression of the ACRB (28) does not converge. This has been explained in Section III-B. For high SNR values, we can approximate the ACRB given in equation (28) by neglecting the second summand containing  $(2\sigma^2)^2$  in the numerator. This approximated average Cramer Rao bound converges also for  $M = 2$  and is in excellent agreement with the values of the MSE of the ML-DF simulations for  $M = 2$  for high SNR values shown on the right hand side of Figure 5.

In summary, we see that the (average) MSE for  $M = 1$  is much larger than the one for  $M = 4$  or  $M = 16$ . The transmit diversity provides a gain of more than 20dB in this respect.

In Figure 6 the Cumulative Density Function (CDF) of the instantenous squared error is shown for  $M = 1, 4$  and  $16$  and a per snapshot SNR of 10dB. The Figure is included to illustrate the match between the outage CRB shown in Figure 4 and the instantenous squared errors of the ML-DF. For example, we find that the 90 per cent

percentile for  $M = 1$  and 4 of the ML-DF in Figure 6 are in perfect agreement with the values of the outage CRB. For  $M = 16$  we find some small deviation, which is due to the limited simulation length.

Moreover, the CDF of the error of the ML-DF illustrates the idea behind using the outage CRB from another perspective. Figure 6 demonstrates that for  $M = 1$  there is a non negligible chance of having a squared error of  $10^{-1}$  or even 1. Assuming a stationary target, this implies that the RCS fluctuations might lead to a situation in which the target cannot be located effectively. For  $M = 4$  and 16 the probability of such a large error is negligible. Thus, we may infer, that particularly for stationary or very slow moving targets, a comparison of different radar systems based solely on the average CRB or the average MSE is not sufficient. A complete evaluation of different systems has to take the slope of the squared error CDF into account. Since the outage CRB,  $\text{CRB}_{out=p}$ , is a lower bound of the  $1 - p$  percentile of any estimator, it is a valid approach to compare systems in this respect.

#### A. Correlated target aspects

We conclude the section presenting simulation results by extending our model to include correlated target aspects. From Figure 1 we infer, that for an insufficient angular separation between the illuminating antennas, the fading coefficients, which determine the returned signal powers from the different transmitters, are not independent. Referring to the signal model discussed in section II, we explore in this section the scenario of non-orthogonal columns  $\mathbf{g}_m$  of the matrix  $\mathbf{G}$ . We approximate this scenario with a first order AR process. For this purpose, the fading vector  $\boldsymbol{\alpha}$  in the signal description in (19) is replaced with  $\boldsymbol{\alpha}'$  which contains  $M$  consecutive samples of an AR process  $u(k)$ , where  $u(k) - \rho \cdot u(k-1) = v(k)$  and  $v(k)$  is a white process with variance  $\sigma^2 = 1 - \rho^2$ . Given that  $\rho$  is real, we find that the correlation matrix  $\mathbf{C}_{\boldsymbol{\alpha}'}$  has the form

$$\mathbf{C}_{\boldsymbol{\alpha}'} = \begin{pmatrix} 1 & \rho & \rho^2 & \dots & \rho^{M-1} \\ \rho & 1 & \rho & & \\ \rho^2 & \rho & 1 & & \vdots \\ \vdots & & & \ddots & \\ \rho^{M-1} & \dots & & & 1 \end{pmatrix}. \quad (34)$$

Using the Cholesky factorization, we find  $\mathbf{A}$  so that  $\mathbf{A}^H \mathbf{A} = \mathbf{C}_{\boldsymbol{\alpha}'}$ . Thus, we may compute  $\boldsymbol{\alpha}'$  using the uncorrelated elements of  $\boldsymbol{\alpha}$  by  $\boldsymbol{\alpha}' = \mathbf{A}^H \boldsymbol{\alpha}$ , as  $\mathbf{C}_{\boldsymbol{\alpha}'} = E\{\boldsymbol{\alpha}' \boldsymbol{\alpha}'^H\} = \mathbf{A}^H E\{\boldsymbol{\alpha} \boldsymbol{\alpha}^H\} \mathbf{A} = \mathbf{A}^H \mathbf{I}_M \mathbf{A}$ .

Figures 7 and 8 show simulation results for correlated target fading among the transmitter aspects for  $M = 4$  and  $M = 16$ , respectively. As expected, for  $\rho = 1$  the performance of the multiple transmitter scenarios degenerates to the one of a single transmitter as all transmitters illuminate actually the same aspect of the target<sup>2</sup>. This is evident when comparing Figures 7 and 8 with Figure 5. Further, the curves for  $\rho = 0$  agree with the curves shown in Figure 5 for  $M = 4$  and  $M = 16$ .

<sup>2</sup>Note, as for  $\rho = 1$  the Cholesky factorization of  $\mathbf{C}_{\boldsymbol{\alpha}'}$  is not possible, the simulations have actually been conducted with  $\rho = 1 - 10^{-8}$  instead of 1.

We see that for  $\rho = 0.9$  and  $\rho = 0.8$  and  $M = 4$  the progression of the curves in Figure 7 is similar to the one for  $M = 2$  in Figure 5. This is expected, as the correlation between the different aspects prevents the full diversity gain. In contrast, the curve for  $\rho = 0.9$  and  $M = 16$  is very close to the curve for  $\rho = 0$ . This is because the two outer transmitters illuminate two aspects which are almost uncorrelated,  $E\{\alpha_1 \alpha_{16}^*\} < 0.2$ . So in other words, full diversity is roughly achieved.

In summary, we can infer from the plots in Figures 7 and 8 that significant gains are possible by employing transmit diversity even when adjacent target aspects result in fading coefficients with correlation coefficients as large as 0.9. Moreover, the difference between the performances for small correlation coefficients, like  $\rho = 0.2$ , and actual orthogonal target aspects is negligible. Therefore, this section underlines again that MIMO radar with transmit diversity is a promising new approach for real world radar systems.

## V. CONCLUSIONS

In this publication we studied MIMO radar as an approach to overcome performance degradations due to the RCS fluctuations. We introduced a signal model, which provides insights into the cause of RCS fluctuations and how to overcome them. We also introduced two theoretical measures to compare the performance of classical and MIMO radar for direction finding, namely the ACRB and the outage CRB. Simulation results further illustrated these measures. The results showed significant gains for MIMO radar. Furthermore, the simulation results for correlated target aspects illustrated that even when full diversity cannot be achieved, MIMO radar still offers significant gains.

We acknowledge that the analysis is carried out for a simplified scenario. However, we showed that MIMO radar is a promising new field of research, and we hope that the analysis introduced in this publication will help explore this field.

## ACKNOWLEDGMENT

The authors would like to thank the anonymous reviewers for their corrections and helpful suggestions improving the quality of this publication. Further, we express our gratitude to Dr. Daniel Fuhrmann for handling the review process.

## REFERENCES

- [1] V. Tarokh, N. Seshadri, and A. Calderbank, "Space-time codes for high data rate wireless communication: Performance criterion and code construction," *IEEE Trans. on Info. Theory*, vol. 44, no. 2, pp. 744–765, March 1998.
- [2] H. Bölcskei and A. J. Paulraj, *The Communications Handbook*, 2nd ed. CRC Press, 2002, ch. Multiple-input multiple-output (MIMO) wireless systems, pp. 90.1 – 90.14.
- [3] E. Fishler, A. H. Haimovich, R. S. Blum, D. Chizhik, L. Cimini, and R. Valenzuela, "MIMO radar: An idea whose time has come," in *Proc. of the IEEE Int. Conf. on Radar*, April 2004.
- [4] E. Fishler, A. H. Haimovich, R. S. Blum, L. Cimini, D. Chizhik, and R. Valenzuela, "Spatial diversity in radars - models and detection performance," *IEEE Trans. on Signal Processing*, vol. 54, no. 3, pp. 823–838, March 2006.
- [5] G. J. Foschini and M. J. Gans, "On Limits of Wireless Communications in a Fading Environment when using multiple Antennas," *Wireless personal Communications*, vol. 6, no. 3, pp. 311–318, March 1998.
- [6] M. Skolnik, *Introduction to Radar Systems*, 2nd ed. McGraw-Hill, 1980.

- [7] D. Baumgarten, "Optimum detection and receiver performance for multistatic radar configurations," in *IEEE Int. Conference on Acoustics, Speech and Signal Processin, ICASSP*, May 1982, pp. 359–362.
- [8] L. Mozzone, S. Bonghi, and F. Filocca, "Diversity in multistatic active sonar," in *Riding the Crest into the 21<sup>st</sup> Century, OCEANS '99, IEEE/MTS*, September 1999.
- [9] T. Johnsen, K. Olsen, S. Johnsrud, and S. R., "Simultaneous use of multiple pseudo random noise codes in multistatic CW radar," in *Proc. of the IEEE Int. Conf. on Radar*, April 2004.
- [10] T. A. Seliga and F. J. Coyne, "Multistatic radar as a means of dealing with the detection of multipath false targets by airport surface detection equipment radars," in *Proc. of the IEEE Int. Conf. on Radar*, May 2003.
- [11] W. Liu, Y. Lu, and J. S. Fu, "A novel threshold optimization for distributed OS-CFAR of multistatic radar systems by using the genetic algorithm," in *Proc. of the IEEE Int. Conf. on Radar*, May 2001.
- [12] D. Rabideau and P. Parker, "Ubiquitous MIMO multifunction digital array radar," in *37<sup>th</sup> Asilomar Conference on Signals, Systems and Computers*, November 2003.
- [13] F. C. Robey, S. Coutts, D. Weikle, J. C. McHarg, and K. Cuomo, "MIMO radar theory and experimental results," in *38<sup>th</sup> Asilomar Conference on Signals, Systems and Computers*, November 2004, pp. 300–304.
- [14] A. Dogandzic and A. Nehorai, "Cramer-Rao bounds for estimating range, velocity, and direction with an active array," *IEEE Transaction on Signal Processing*, vol. 49, no. 6, pp. 1122–1137, June 2001.
- [15] S. Pasupathy and A. N. Venetsanopoulos, "Optimum active array processing structure and space-time factorability," *IEEE Trans. Aerosp. Electron. Syst.*, vol. 10, pp. 770–778, 1974.
- [16] L. Swindlehurst and P. Stoica, "Maximum likelihood methods in radar array signal processing," *Proc. of the IEEE*, vol. 86, no. 2, pp. 421–441, Feb. 1998.
- [17] S. Haykin, J. Litva, and T. J. Shepherd, *Radar Array Processing*, 1st ed. New York: Springer - Verlag, 1993.
- [18] J. Ward, "Cramer-Rao bounds for target angle and Doppler estimation with space-time adaptive processing radar," in *Proc. 29<sup>th</sup> Asilomar Conf. Signals, Syst. Comput.*, Nov. 1995, pp. 1198–1202.
- [19] F. Gesbert, H. Bölcskei, D. A. Gore, and A. J. Paulraj, "Outdoor MIMO wireless channels: Models and Performance Prediction," *IEEE Trans. on Commun.*, vol. 50, no. 12, pp. 1926–1934, December 2002.
- [20] P. E. Howland, "Target tracking using television-based bistatic radar," *IEE Proc., Radar Sonar Navig.*, vol. 146, no. 3, pp. 166–174, June 1999.
- [21] —, "Passive Tracking of Airborne Targets using only Doppler and DOA Information," *IEE Colloquium on Alg. for Target Tracking*, pp. 37–39, May 1995.
- [22] P. Stoica, E. G. Larsson, and A. B. Gershman, "The Stochastic CRB for Array Processing: Textbook Derivation," *IEEE Signal Processing Letters*, vol. 8, no. 5, pp. 148–150, May 2001.
- [23] H. L. V. Trees, *Optimum Array Processing*, 1st ed. John Wiley, 2003.
- [24] A. Papoulis, *Probability, Random Variables and Stochastic Processes*, 3rd ed. Mc Graw Hill, 1991.

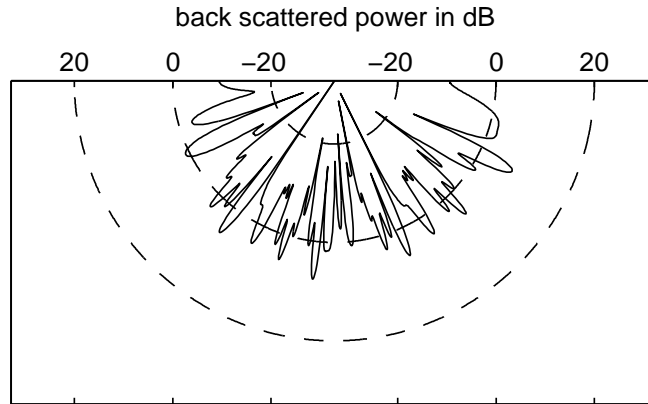


Fig. 1. Reflected power in dB at  $\theta = 0$  when illuminating from different angles.

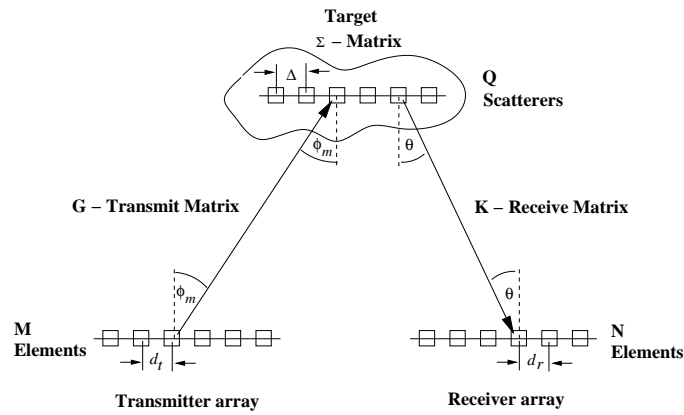


Fig. 2. Bistatic radar scenario. The target consists of multiple scatterers organized in the form of a linear array.

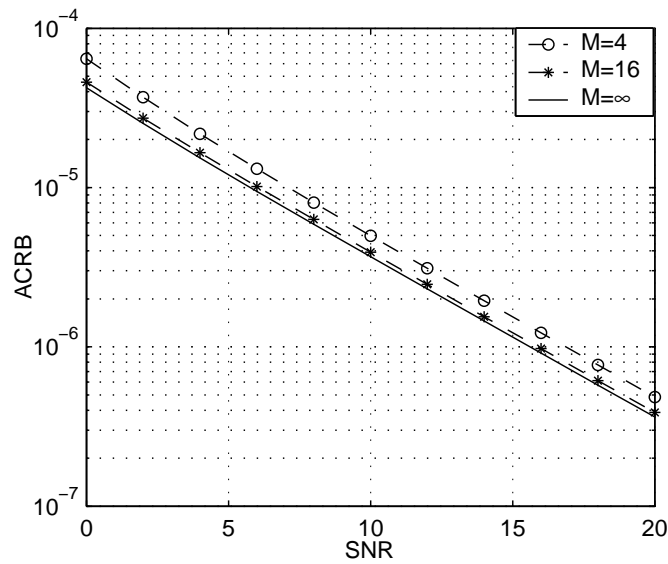


Fig. 3. Average CRB versus SNR.

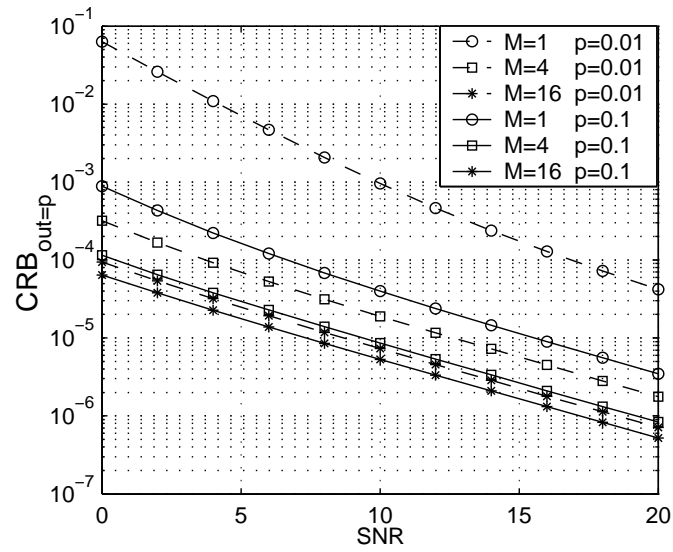


Fig. 4. Outage CRB versus SNR.

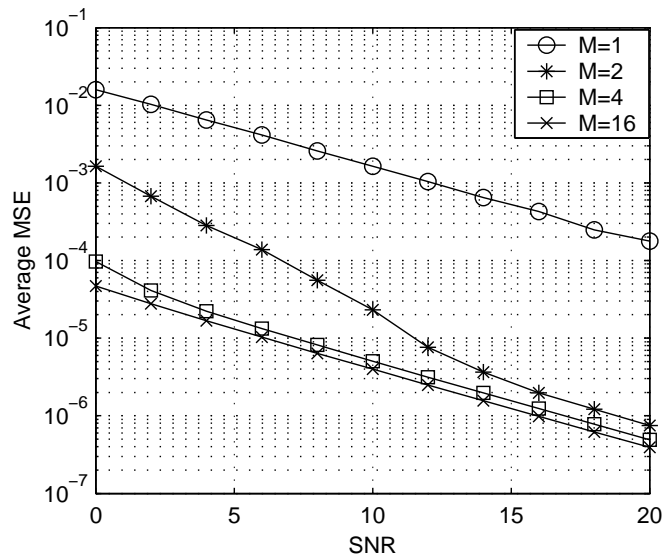


Fig. 5. Average MSE of the ML estimator versus SNR

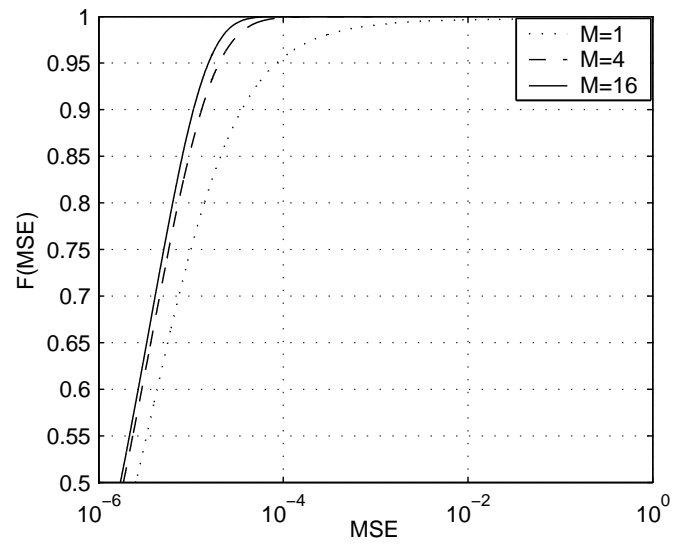


Fig. 6. CDF of the instantaneous error for  $M = 1, 4, 16$  at  $SNR = 10\text{dB}$ .

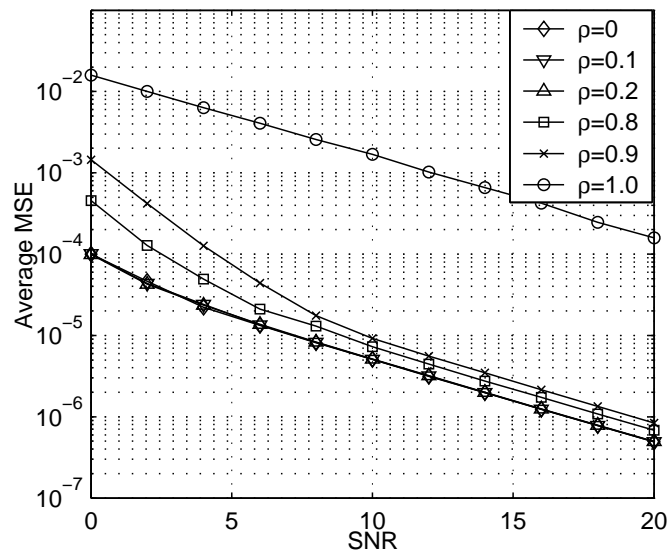


Fig. 7. Average MSE for correlated target aspects and  $M = 4$ .

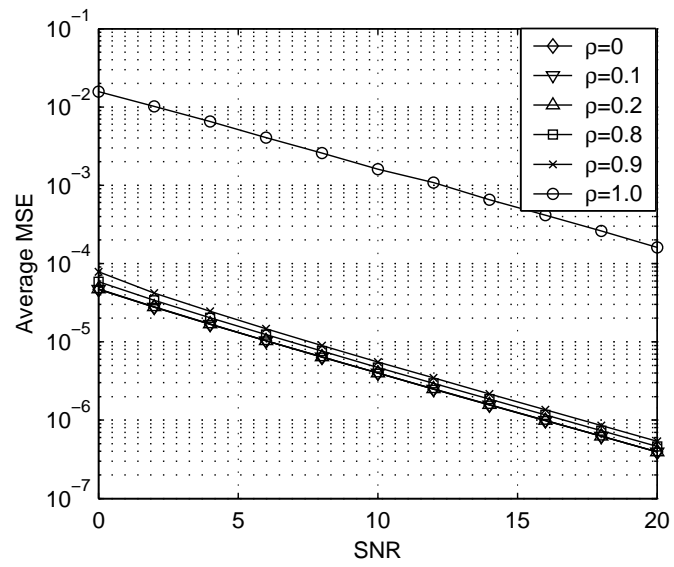


Fig. 8. Average MSE for correlated target aspects and  $M=16$ .